A new three-dimensional cobalt phosphate: $Co_5(OH_2)_4(HPO_4)_2(PO_4)_2$

Zhangang Han[a],*, Aixiang Tian[b], Jun Peng[b],**, Xueliang Zhai[a]

[a]Faculty of Chemistry, Hebei Normal University, Shijiazhuang, Hebei 050016, PR China
[b]Faculty of Chemistry, Northeast Normal University, Changchun, Jilin 130024, PR China

Abstract

A three-dimensional (3D) cobalt phosphate: $Co_5(OH_2)_4(HPO_4)_2(PO_4)_2$ (**1**), has been synthesized by hydrothermal reaction and characterized by single-crystal X-ray diffraction, thermogravimetric analysis, and magnetic techniques. The title compound is a template free cobalt phosphate. Compound **1** exhibits a complex net architecture based on edge- and corner-sharing of CoO_6 and PO_4 polyhedra. The magnetic susceptibility measurements indicated that the title compound obeys Curie–Weiss behavior down to a temperature of 17 K at which an antiferromagnetic phase transition occurs.
© 2006 Elsevier Inc. All rights reserved.

Keywords: Cobalt; Phosphate; Metal-phosphate; Magnetism

1. Introduction

The metal-phosphate chemistry has attracted intensive attention because of their extensive application as heterogeneous catalysts [1,2], sorbents and ion exchangers [3]. There are several systems in this field, such as V–P–O, Zn–P–O, Fe–P–O, Co–P–O, Mo–P–O, M–Co–P–O ($M = $ Na, K, Rb, Cs, and NH_4^+) and so on. Since the use of structure-directing organic molecules has evolved into a successful strategy for the synthesis of new materials, the metal-phosphate family has been further exploited. Much work has been focused on cobalt phosphates owing to its feasibility for tetrahedral and octahedral coordination and potential catalytic properties [4–15]. A detailed review with regard to cobalt phosphates provided some insight into the structures of metal-phosphate chemistry, especially linkage modes based on the corresponding M/P polyhedra [12,13]. In this paper, we report the synthesis and characterization of a new three-dimensional (3D) structure: $Co_5(OH_2)_4(HPO_4)_2(PO_4)_2$ (**1**).

2. Experimental section

2.1. Synthesis

Compound **1** was synthesized from a mixed solution of $Co(NO_3)_2$ and H_3PO_4 with a molar ratio of 2:1. The resulting solution was transferred into a 20 mL Teflon-lined autoclave after it was stirred for ca. 20 min in air. The reaction vessel was filled to 70% volume capacity. Then the reactor was heated under autogenous pressure at 175 °C for 4 days. After slow cooling (10 °C/h) to room temperature, pink needlelike crystals were obtained. The crystals were picked out manually, washed with distilled water, and air-dried at 50 °C. IR data (cm^{-1}): 430(w), 520(w), 810(m), 881(m), 1078(s).

2.2. X-ray crystallography

A crystal of compound **1** with dimension $0.311 \times 0.121 \times 0.086\ mm^3$ was glued on a glass fiber. Data were collected on a Rigaku R-AXIS RAPID IP imaging-plate X-ray diffractometer with Mo$K\alpha$ monochromated radiation ($\lambda = 0.71703\ \text{Å}$) at 293 K. Data were corrected for Lorentz and polarization effects, and an empirical absorption correction was applied. The structure for compound **1** was solved by direct method and refined by

*Corresponding author.
**Also to be corresponded.
E-mail addresses: hanzg116@yahoo.com.cn (Z. Han), jpeng@nenu.edu.cn (J. Peng).

the full-matrix least-squares methods on F^2 using the SHELXTL crystallographic software package [16]. Anisotropic thermal parameters were used to refine all non-hydrogen atoms. The hydrogen atoms were located from difference Fourier maps. The crystallographic data and selected bond lengths were listed in Tables 1 and 2; atomic coordinates and selected bond angles of compound **1** were provided in STables 1 and 2, respectively.

3. Results and discussion

3.1. Crystal structure

The X-ray single-crystal analysis revealed that compound **1** consists of a 3D network constructed from CoO_6

Table 1
Crystal data and structure refinement for compound **1**

Chemical formula	Co5 H10 O20 P4
Formula weight	748.61
Temperature	293(2) K
Wavelength	0.71073 Å
Crystal system, space group	Monoclinic, C2/c
Unit cell dimensions	$a = 17.263(4)$ Å, $\alpha = 90°$
	$b = 8.9091(18)$ Å, $\beta = 96.46(3)°$
	$c = 9.3154(19)$ Å, $\gamma = 90°$
Volume	1423.6(5) Å^3
Z, calculated density	4, 3.493 Mg/m^3
Absorption coefficient	6.279 mm^{-1}
$F(000)$	1460
Crystal size	$0.311 \times 0.121 \times 0.086$ mm
Theta range for data collection	3.30–27.46°.
Limiting indices	$-22 \leqslant h \leqslant 22, -11 \leqslant k \leqslant 11,$
	$-11 \leqslant l \leqslant 12$
Reflections collected/unique	6671/1633 [R(int) = 0.0213]
Completeness to $\theta = 27.46°$	99.70%
Absorption correction	Empirical
Max. and min. transmission	0.583 and 0.428
Refinement method	Full-matrix least-squares on F^2
Data/restraints/parameters	1633/0/152
Goodness-of-fit on F^2	1.042
Final R indices [$I > 2\mathrm{sigma}(I)$]	$R_1 = 0.0200$, w$R_2 = 0.0481$
R indices (all data)	$R_1 = 0.0223$, w$R_2 = 0.0489$
Largest diff. peak and hole	0.466 and -0.559 e Å^{-3}

octahedra and PO$_4$ tetrahedra via corner- and edge-sharing. The title compound is a template free cobalt phosphate and has a formula $Co_5(OH_2)_4(HPO_4)_2(PO_4)_2$. Charge neutrality of the overall structure is achieved by the incorporation of the hydrogen atoms of coordination water molecule and hydroxyl groups. The asymmetric unit is represented on Fig. 1.

Each of three crystallographically independent Co(II) atoms has octahedral coordination geometry, being coordinated by six oxygen atoms with cobalt oxygen (Co–O) lengths in the range 2.010(2)–2.286(1) Å. It should be point out that two coordinated water molecules: O(6) and O(7) have different linkage modes: μ_2-O(6) bridges two Co octahedra, while μ_1-O(7) serves as a pendant aqua. Among two crystallographically independent PO$_4$ groups, P(2) tetrahedron acts a quadridentate ligand in coordination with four Co atoms, while P(1) tetrahedron functions as a tridentate mode to bridge three Co atoms, the remaining fourth oxygen O(10) is a hydroxyl group. The geometry of PO$_4$ groups is almost regular with the distance of P–O bond in the range 1.522(1)–1.552(1) Å, the only marked deviation being to accommodate the P–O–H group. The extension of P(1)–O(10) bond to 1.561(1) Å is typical of such linkage, confirming the location of H(5) atom.

The polyhedral connectivity built upon CoO$_6$ and PO$_4$ units leads to the formation of an infinite 3D network.
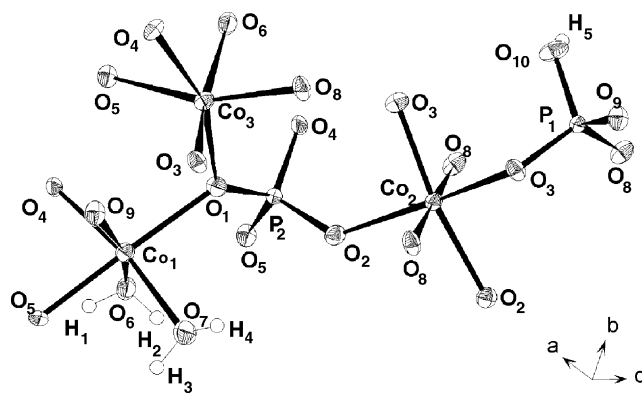

Fig. 1. ORTEP drawing of compound **1** showing the labels of atoms with thermal ellipsoids at 75% probability.

Table 2
Bond lengths (Å) for compound **1**

Co(1)–O(7)	2.010(2)	Co(2)–O(8)#3	2.180(2)	P(1)–O(10)	1.561(2)
Co(1)–O(4)	2.036(2)	Co(3)–O(4)#4	2.068(1)	P(2)–O(5)#7	1.527(2)
Co(1)–O(9)	2.095(1)	Co(3)–O(1)	2.072(1)	P(2)–O(4)#6	1.541(2)
Co(1)–O(5)	2.122(1)	Co(3)–O(8)#1	2.122(2)	P(2)–O(2)	1.552(1)
Co(1)–O(6)	2.184(2)	Co(3)–O(3)#5	2.123(1)	P(2)–O(1)	1.552(1)
Co(1)–O(1)	2.203(1)	Co(3)–O(6)#6	2.159(2)	O(6)–H(1)	0.80(5)
Co(2)–O(3)#1	2.050(1)	Co(3)–O(5)#4	2.286(1)	O(6)–H(2)	0.84(5)
Co(2)–O(3)	2.050(1)	P(1)–O(3)	1.522(1)	O(7)–H(3)	0.91(5)
Co(2)–O(2)	2.172(1)	P(1)–O(9)#5	1.529(1)	O(7)–H(4)	0.81(4)
Co(2)–O(2)#1	2.172(1)	P(1)–O(8)	1.531(1)	O(10)–H(5)	0.77(4)
Co(2)–O(8)#2	2.180(2)				

Symmetry transformations used to generate equivalent atoms: #1$-x, y, -z+5/2$; #2$-x, -y+1, -z+3$; #3 $x, -y+1, z-1/2$; #4$-x+1/2, y+1/2, -z+3/2$; #5$-x, -y+1, -z+2$; #6$-x+1/2, -y+1/2, -z+2$; #7 $x, -y, z+1/2$.

To simplify the analysis, the pentamer of CoO_6 (linked by broken lines) based on the formula can be seen as a building unit (see Fig. 2). Fig. 2a shows a 2D layer built up by the arrangement of pentamers. Fig. 2b is a side view of the layer along the b axis. Fig. 2c presents a 3D structure formed by these layers, in which only Co atoms of the pentamer are drawn while other atoms are omitted for clarity. In this view, the framework is built from identical layers and these layers are staggered. Fig. 3 represents distinctly the corner- and edge-sharing of CoO_6 and PO_4 polyhedra. Inspection of the interpolyhedral oxygen–oxygen distances (see STable 3) shows that the extensive hydrogen bond interaction occurs among hydroxyl, water molecules and bridging oxygens (see Fig. 4), which further strengthen the stability of compound 1.

It is of interest to compare the other hydrous cobalt phosphate compounds with high Co and P ratio with 1, such as $Co_3(PO_4)_2 \cdot 2H_2O$ (2) [17] and $Co_7(PO_4)_2(HPO_4)_4$ (3) [18]. Three compounds not only differ in the ratio of Co:P and the coordination geometry of cobalt cation (only octahedral in 1, octahedral and bipyramidal in 2 and 3), but also differ in the framework connectivity. Moreover,

three compounds have also different space group symmetry (C2/c for 1, P2(1)/c for 2 and P-1 for 3). All these demonstrate the structural diversity of Co–P chemistry.

Bond valence sum (BVS) calculations [19] give the values for Co(1) 1.983, Co(2) 1.840, and Co(3) 1.829, indicating all cobalt atoms exist in the divalent state. The values for P(1) and P(2) are 4.814 and 4.719, indicating P atoms are in the $+5$ oxidative state. The values for oxygen atoms fall in three classes: O(1) 1.760, O(2) 1.697, O(3) 2.318, O(4) 1.943, O(5) 1.745, O(8) 2.066 and O(9) 1.561, have bond strength sums near two; the values for O(6) and O(7) are 0.548 and 0.423 (the hydrogen atoms have not been included), respectively. Although having different environments, the calculation sums indicate that O(6) and O(7) are water molecules; O(10) possesses a bond strength sum near one (1.125), indicating that it be a hydroxyl oxygen. These results further confirm the title compound's formula. The existence of these hydrogen atoms maintains the necessary charge balance.

In the IR spectrum of compound 1, the peaks at 430, 520, 810 and 881 cm^{-1} are attributed to $Co-O_a$ asymmetric vibrations (O_a = terminal oxygen or bridged oxygen). The
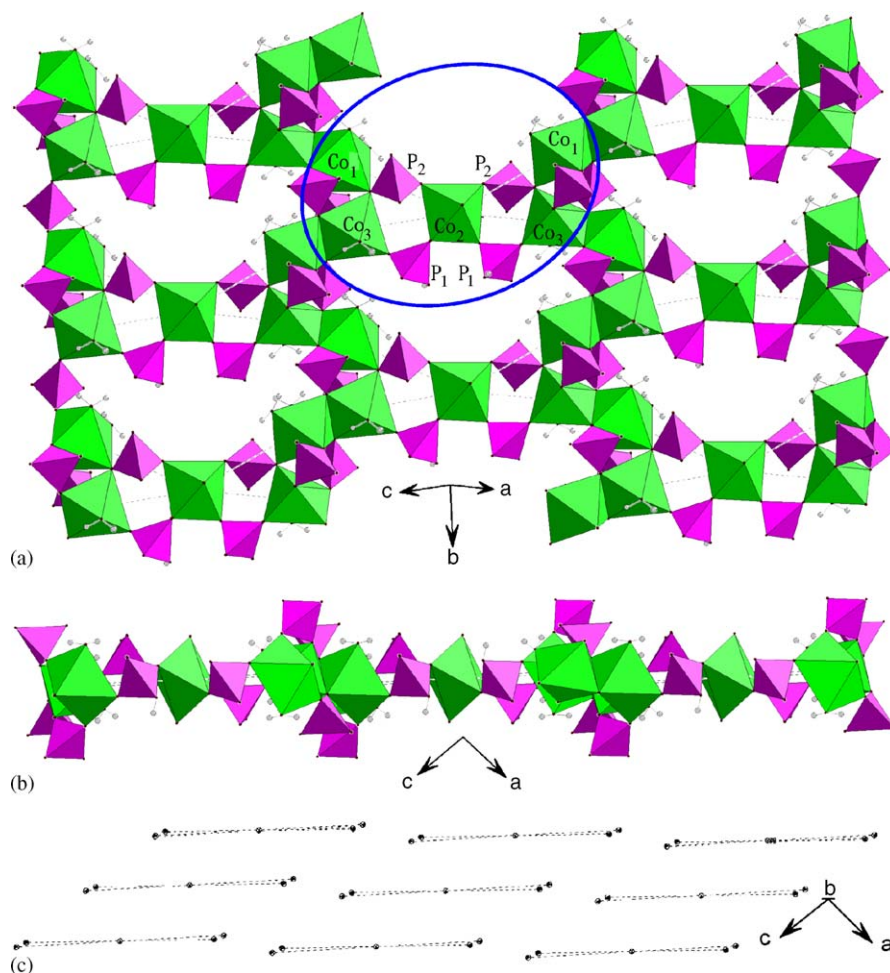

Fig. 2. The arrangement of CoO_6 (green) and PO_4 (pink) (dashed and ellipse: pentamer of CoO_6): (a) a two-dimensional (2D) layer view; (b) a side view of the 2D layer; (c) a 3D view in which only Co atoms of the pentamer are drawn while other atoms are omitted for clarity.
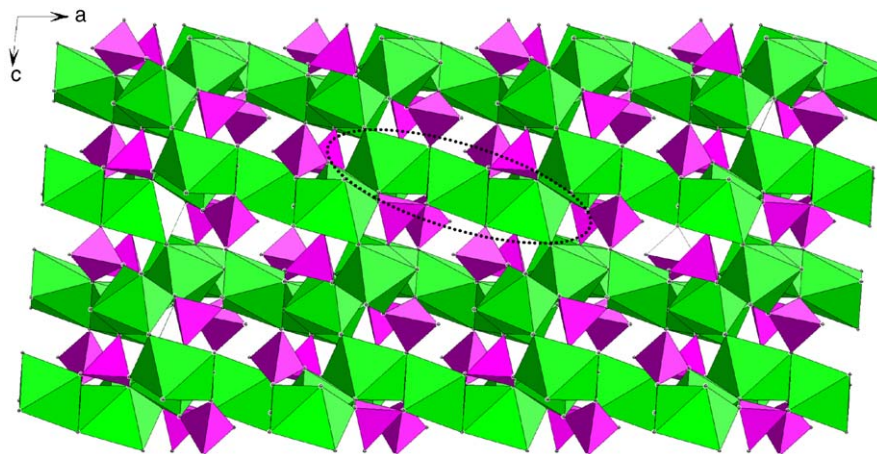
Fig. 3. The polyhedral representation of **1** exhibiting that the 3D framework is fabricated from CoO_6 and PO_4 polyhedra.
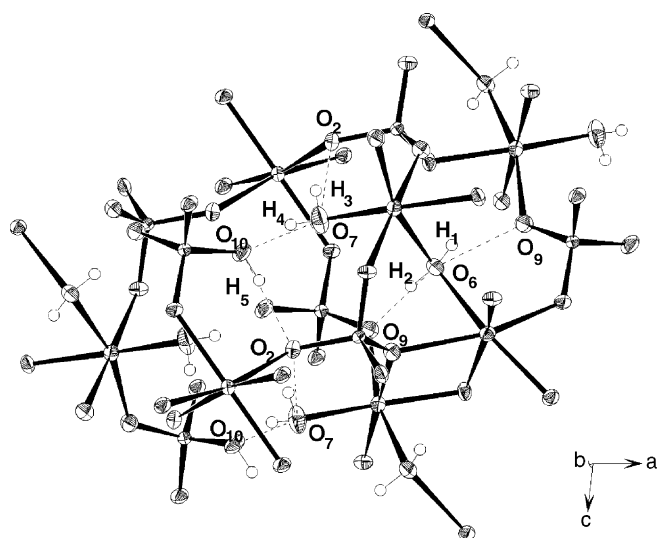

Fig. 4. A view showing the hydrogen bonding linkage in **1**.

strong peak at $1078 \, cm^{-1}$ is attributed to P–O stretching vibration.

Thermal analysis (TGA-DTA) was carried out under a nitrogen atmosphere from 30 to 1000 °C, and the results are presented in SFig. 1. The TGA curve shows two steps: a slow mass loss (ca. 0.02%) ranging from 220 to 490 °C and a sharp mass loss (ca. 7.861%) ranging from 490 to 540 °C, attributing to the removal of water, including coordinated water and being formed by the condensation of HO–P groups. The total weight loss (7.881%) is consistent with the theoretical value (8.407%). XRD measurement identified that the TGA experimental residua are mixture phases of α-$Co_2P_2O_7$ and Co_3O_4 (see SFig. 2). The DTA curve reveals three endothermic peaks at 526, 680 and 700 °C, corresponding to the loss of water and/or a phase transformation of cobalt phosphate, respectively.

The extensive –Co–O–Co– linkages in compound **1** drive us to research its magnetic behavior. Several compounds containing –Co–O–Co– linkages show paramagnetic behavior at higher temperatures and antiferromagnetic transition on cooling. For example, $Co_2(OH)PO_4$ [13], $NaCoPO_4(P2_1/c)$ [4(b)], and $NaCoPO_4$ (*Pnma*) [4(c)] containing edge-sharing octahedral chains have antiferromagnetic transition at 70, 15, and 25 K, respectively. Compound **1** shows similar magnetic behavior. The variable temperature magnetic susceptibility for **1** is shown in Fig. 5. The linear behavior of $1/\chi(T)$ obeys well the Curie–Weiss equation ($C = 15.0 \, emu \, K/mol$, $\theta = -15.8 \, K$) above 17 K at which the sample turns antiferromagnetic. Thus, the maximum in the magnetic susceptibility is observed at 17 K. The effective magnetic moment per metal atom at 300 K, $4.26 \, \mu_B$, is greater than the spin-only value ($3.87 \, \mu_B$), indicating the existence of a significant orbital contribution, which is commonly found in cobalt compounds. Below, 17 K the inverse molar susceptibility curve rises abruptly with a maximum at ca. 5 K and then decreases sharply, which is likely due to the presence of a small amount of paramagnetic impurities. The negative Weiss temperature is characteristic of an antiferromagnetic interaction that is verified by χT vs. T curve too. A clear kink on the χT vs. T curve around 220 K may be ascribed to a slight distortion of –Co–O–Co– network in **1**.

4. Conclusions

A 3D cobalt phosphate: $Co_5(OH_2)_4(HPO_4)_2(PO_4)_2$ (**1**), has been prepared and characterized. Compound **1** exhibits a complex net architecture based on CoO_6 octahedra and PO_4 tetrahedra and is pretty condensed. The necessary charge balance is maintained by the incorporation of H atoms of coordination water and hydroxyl groups. The magnetic susceptibility measurements showed that compound **1** obeys Curie–Weiss behavior down to a temperature of 17 K at which an antiferromagnetic phase transition occurs.
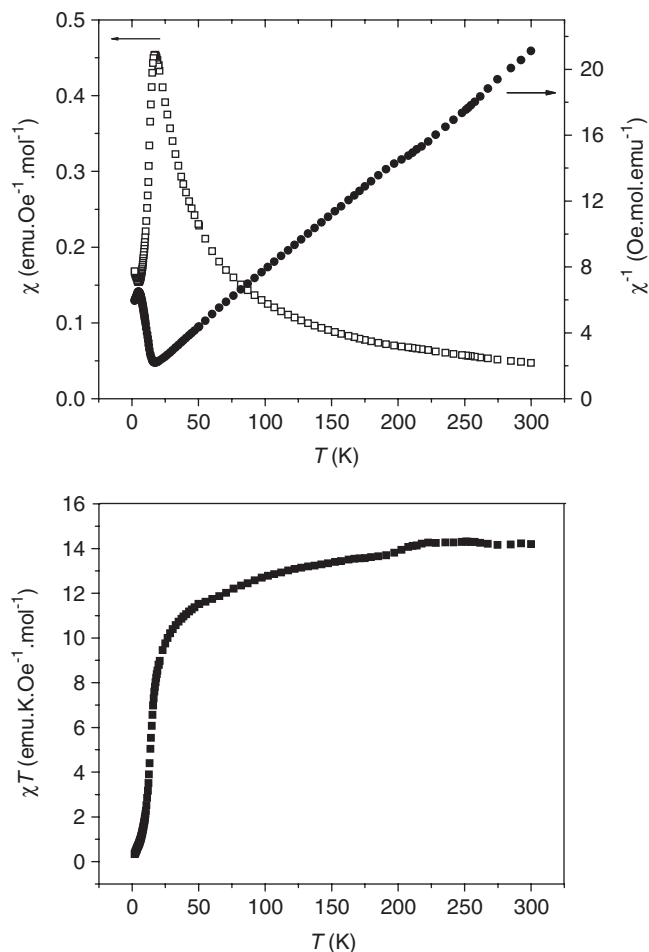
Fig. 5. Temperature-dependent magnetic susceptibility data for **1**: χ, χ^{-1} and χT plotted as a function of temperature over the 2–300 K region.

Appendix A. Supplementary data

Supplementary data associated with this article can be found in the online version at doi:10.1016/j.jssc.2006.05.014.

References

[1] G. Centi, Catal. Today 16 (1993) 1.
[2] I.J. Ellison, G.J. Hutchings, M.T. Sananes, J.C. Volta, J. Chem. Soc. Chem. Commun. (1994) 1093.
[3] (a) A. Clearfield, Chem. Rev. 88 (1988) 125;
    (b) S.L. Suib, Chem. Rev. 93 (1993) 803.
[4] (a) P. Feng, X. Bu, S.H. Tolbert, G.D. Stucky, J. Am. Chem. Soc. 119 (1997) 2497;
    (b) P. Feng, X. Bu, G.D. Stucky, J. Solid State Chem. 129 (1997) 328;
    (c) P. Feng, X. Bu, G.D. Stucky, J. Solid State Chem. 131 (1997) 160.
[5] (a) X. Bu, P. Feng, T.E. Gier, G.D. Stucky, J. Solid State Chem. 136 (1998) 210;
    (b) P. Feng, X. Bu, G.D. Stucky, Nature 388 (1997) 735.
[6] X. Bu, P. Feng, G.D. Stucky, Science 278 (1997) 2080.
[7] (a) J.R.D. DeBord, R.C. Haushalter, J. Zubieta, J. Solid State Chem. 125 (1996) 270;
    (b) A. Choudhury, S. Natarajan, C.N.R. Rao, J. Solid State Chem. 155 (2000) 62–70.
[8] A.R. Cowley, A.M. Chippindale, J. Chem. Soc. Dalton Trans. (1999) 2147.
[9] C.N.R. Rao, S. Natarajan, S. Neeraj, J. Am. Chem. Soc. 122 (2000) 2810.
[10] S. Natarajan, S. Neeraj, A. Choudhury, C.N.R. Rao, Inorg. Chem. 39 (2000) 1426.
[11] H.-M. Yuan, J.-S. Chen, G.-S. Zhu, J.-Y. Li, J.-H. Yu, G.-D. Yang, R.-R. Xu, Inorg. Chem. 39 (2000) 1476.
[12] R.P. Bontchev, M.N. Iliev, L.M. Dezaneti, A.J. Jacobson, Solid State Sci. 3 (2001) 133–142.
[13] X. Bu, P. Feng, G.D. Stucky, J. Solid State Chem. 131 (1997) 387.
[14] H. Effenberger, R. Parik, F. Pertlik, B. Rieck, Z. Kristallogr. 194 (1991) 199.
[15] D. Tranqui, A. Durif, J.C. Guitel, M.T. Averbuch-Pouchot, Bull. Soc. Chim. Fr. 1759 (1968) 1968.
[16] (a) G.M. Sheldrick, SHELXS 97: Programs for Crystal Structure Solution, University of Göttingen, Germany, 1997;
    (b) G.M. Sheldrick, SHELXL 97: Programs for Crystal Structure Refinement, University of Göttingen, Germany, 1997.
[17] J.B. Anderson, E. Kostiner, F.A. Ruszala, Inorg. Chem. 15 (11) (1976) 2744.
[18] P. Lightfoot, A.K. Chfftham, Acta Crystallogr. C 44 (1988) 1331.
[19] I.D. Brown, D. Altermatt, Acta Crystallogr. B. 41 (1985) 244.